Pergamon

Materials Research Bulletin, Vol. 34, No. 7, pp. 1055–1064, 1999

PII S0025-5408(99)00103-8

PREPARATION OF MICROPOROUS NICKEL ELECTRODEPOSITS USING A POLYMER MATRIX

I.J. Brown, D. Clift, and S. Sotiropoulos*
School of Chemical, Environmental, and Mining Engineering, Nottingham University,
University Park, Nottingham NG7 2RD, UK

(Refereed)
(Received July 15, 1998; Accepted September 11, 1998)

ABSTRACT

Nickel-mesh electrodes were embedded into polyHIPE (a generic hollow fiber polymer) by immersion in the precursor emulsion and subsequent entrapment into the solid microporous matrix produced by polymerization and drying. Immersing this Ni/polyHIPE/Ni composite into a nickel electroplating bath and passing direct current through the two electrodes resulted in growing Ni electrodeposits on the cathode and through the polymer cells and pores. When the polymer matrix was subsequently burned off, a granular microporous Ni coating was produced on the cathode. Variation of the electroplating time and current density showed that the structure of the Ni coating is determined by the local distortions of the electric field inside the tortuous microporous body of the insulating polymer. *© 1999 Elsevier Science Ltd*

KEYWORDS: A. metals, A. microporous materials, C. electrochemical measurements, C. electron microscopy, D. microstructure

INTRODUCTION

The preparation of high surface area Ni electrode materials is relevant to a number of industrial applications of electrochemical technology. The most important applications include the use of Ni hydrogen anodes in alkaline or molten carbonate H_2/O_2 fuel cells [1–4],

---

*To whom correspondence should be addressed. Tel: +44-115-9514182. Fax: +44-115-9514181. E-mail: s.sotiropoulos@nottingham.ac.uk.

NiO(OH)/NiO cathodes in nickel–cadmium and nickel–hydrogen batteries [5,6] and hydrogen-evolving Ni cathodes in alkaline water electrolysis [7,8]. Nickel foam electrodes have been successfully used as three-dimensional porous electrodes in the electrolytic recovery of Cu ions [9] (wastewater treatment) and in electroorganic synthesis [10,11], and Raney nickel electrodes have been employed in the electrochemical hydrogenation of organics [12,13].

There are various types of high surface area Ni electrodes and many different methods used for their preparation. Sintered microporous Ni coatings on electrodes are usually prepared according to the ceramic foil-casting technology by a procedure that involves mixing of a micrometer-size nickel powder with an organic binder, which is subsequently thermally decomposed, and further sintering at elevated temperatures in a hydrogen atmosphere [4]. Techniques used in the production of reticulated metal include the incorporation of the metal into a porous matrix and subsequent matrix decomposition [14] or the use of foaming agents [15]. Highly porous metal structures can also be obtained by sintering metal microfibers [6,16,17]. Various methods for the production of nanoporous Ni coatings, including cold rolling, plasma spraying, annealing, and cathodic codeposition of the Raney nickel precursor alloys (Ni/Al or Ni/Zn) on a nickel support, are reviewed in ref. 18. Smooth Raney nickel coatings have also been produced by sherardizing of nickel substrates, i.e., by the reaction of Ni with Zn vapors at 400°C, which results in the formation of a smooth Ni/Zn precursor coating [19].

PolyHIPE polymer (PHP) is a microporous material developed at Unilever [20] and Los Alamos National Laboratories [21] and used since by a number of research groups [22,23]. It is produced through the formation of a high internal phase water-in-oil emulsion, in which the volume of the aqueous dispersed phase is greater than about 75%, and the subsequent polymerization (at 60°C) of the oil phase, which contains the monomer styrene (and occasionally other monomers) and the cross-linker divinyl benzene. This results in the production of a polymer matrix with an extremely high void (up to 97%) due to the evaporation of the water droplets, which were present in the precursor emulsion. The structure of PHP, therefore, is characterized by the presence of numerous cells (1–100 μm

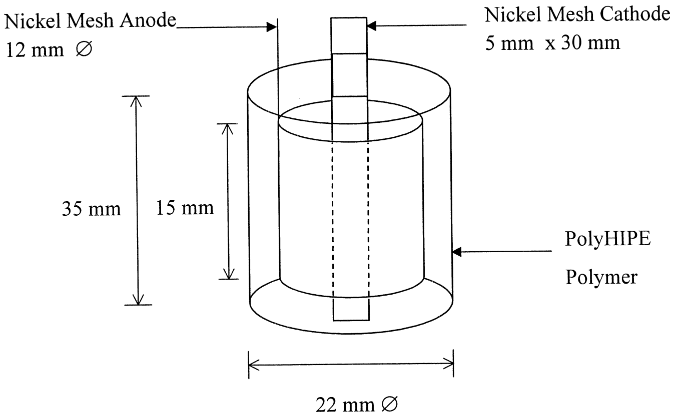

FIG. 1
Schematic representation of the electroplating cell comprised of a rectangular Ni-mesh cathode and a cylindrical Ni-mesh anode, embedded in a polyHIPE polymer body.

diameter) interconnected by small pores (0.1–10 μm diameter). The size of both the cells and the pores can be controlled by changing the mixing time, the surfactant (emulsion stabilizer) concentration, and the monomer composition during the emulsification.

In a recent paper [24], we reported for the first time the successful incorporation of Ni into the PHP matrix by electroplating through its pores and onto a thin Au-layer electrode pasted on one side of a polymer sample. Burnout of the polymer resulted in a granular Ni structure of a very high BET surface area (50 m^2g^{-1}). Those preliminary experiments were useful in establishing the viability of the method, but their logical extension to cases of industrial interest would be the application of the method to the production of porous Ni coatings onto Ni or stainless steel electrodes. The work presented here introduces a modification of the technique, whereby the Ni cathode (together with a Ni anode) is immersed into the precursor emulsion and finally entrapped in the PHP body after polymerization. The Ni-cathode/PHP/Ni-anode composite cell is then used in a Ni electroplating bath, and Ni is deposited through the polymer pores onto the cathode. The effect of the electroplating current density and duration on the resulting Ni coating (after polymer burnout) is also investigated.

EXPERIMENTAL

Preparation of Ni/polyHIPE Polymer/Ni Composite Electrochemical Cells. In this work, polymer of an 80% void was produced; a typical production batch consisted of 500 ml of emulsion, prepared by mixing 400 ml of water phase with 100 ml of oil phase. The composition of the oil phase for the preparation of elastomeric polyHIPE was (by volume): 15% styrene (Aldrich, 99%), 62% 2-ethylhexyl acrylate (Aldrich), 8% divinyl benzene (Aldrich, 80%), and 15% sorbitan monooeleate (Aldrich, 95%). The aqueous phase was distilled water and 1% w/w potassium persulfate (Aldrich, 99+%), which acted as the polymerization initiator. The emulsion was produced in a stainless steel mixing vessel equipped with a Janke and Kunkel (IKA Labortechnik) RW 20DZM two-blade mixer, according to the procedure described elsewhere [24]. The emulsion was then poured into glass vials, and a rectangular Ni-mesh cathode (26 × 26 wires 0.25 mm thick per inch, Goodfellow Ltd) of typical apparent areas of 1–1.5 cm^2, together with a cylindrical piece of the same mesh serving as the anode, was immersed in the emulsion. The inter-electrode gap was typically in the 3.5–6 mm range. Two mesh strips protruding from each electrode and out of the emulsion were subsequently used to make electrical contacts to the electrodes. The entire assembly was then covered tightly with parafilm to minimize water evaporation during polymerization, which was performed for 6 h in an oven heated at 60°C. After polymerization had been completed, the cover was removed and the samples remained in the oven at 60°C for another 24 h to remove residual water from the pores. The sorbitan monooleate, which was the surfactant used as an emulsion stabilizer, was removed by washing several times with boiling isopropyl alcohol. The Ni/PHP/Ni composite cell prepared as a result of this procedure is depicted in Figure 1, in which typical dimensions are also shown.

Ni Electrodeposition. A standard nickel sulfamate bath [25] served as the electroplating solution at 60°C: 600 g/l nickel sulfamate (Aldrich, 98%), 10 g/l nickel chloride (Aldrich), and 40 g/l boric acid (Aldrich, 99.5+%). A regulated 7A-35V DC GW(GPR-3060) laboratory power supply was used to carry out the electroplating at various current densities in the 3–300 mA cm^{-2} range. The current densities are reported per apparent area of the Ni mesh (one face). A 1.6 cm^2 true geometric electrode area per 1 cm^2 apparent mesh area of the Ni

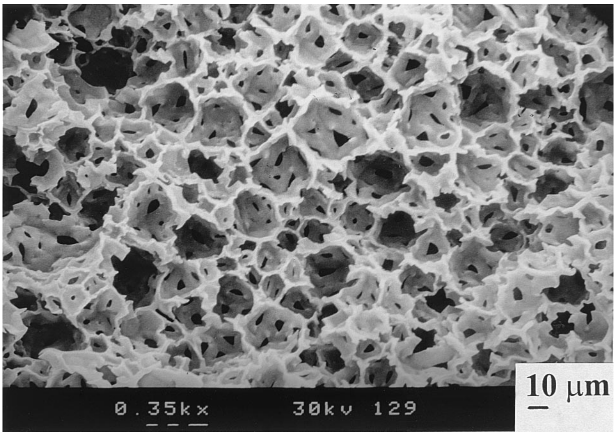

FIG. 2
SEM micrograph of a cross section of a plain polyHIPE sample.

wire in the cathode mesh (two faces, due to the anode surrounding the cathode) was estimated from the manufacturer's specifications and SEM photographs. Hence, all current densities reported hereafter should be divided by 1.6 to give the true current density. Prior to electroplating, the Ni electrodes were activated by immersion into a 1:1 HCl–water solution for a few minutes.

Burnout of the Polymer Matrix and SEM Analysis. The burnout of the polymeric matrix of the Ni/PHP/Ni composites after electroplating was carried out under air atmosphere in a preheated furnace at 500°C for 1 h. SEM and EDAX analyses of the resulting material have confirmed the complete polymer burnout at the end of this procedure [24]. SEM experiments were carried out with a Hitachi S-570.

RESULTS AND DISCUSSION

Figure 2 shows the SEM micrograph of polyHIPE polymer before plating, in which a regular structure of closed but porous cells can readily be seen. The polymer structure consisted of large cells of a 10–30-μm diameter, corresponding to the water droplets of the initial water-in-oil emulsion, interconnected by smaller pores of a 3–5-μm diameter, corresponding to the contact areas of the initially present water droplets.

Figure 3(a) shows the micrograph of the Ni-mesh cathode prior to its incorporation into the polymer body and electroplating. Figure 3(b) shows that of the cathode mesh coated with a Ni electrodeposit following electroplating for 24 h at a rate of 35 mA cm^{-2} in a nickel sulfamate bath and after the polymer matrix of the resulting composite had been thermally decomposed. It can be seen that a uniform microporous Ni coating was produced on the Ni cathode. The electrodeposit appears to have a cauliflower structure organized in near-spherical interconnected aggregates of 150–50 μm diameter, which consist of smaller spherical deposits. Although the presence of the polymer in contact with the cathode is certainly responsible for the structure of the microporous deposit (electroplating of plain Ni mesh at same current densities results in nonporous homogeneous coatings), there is no

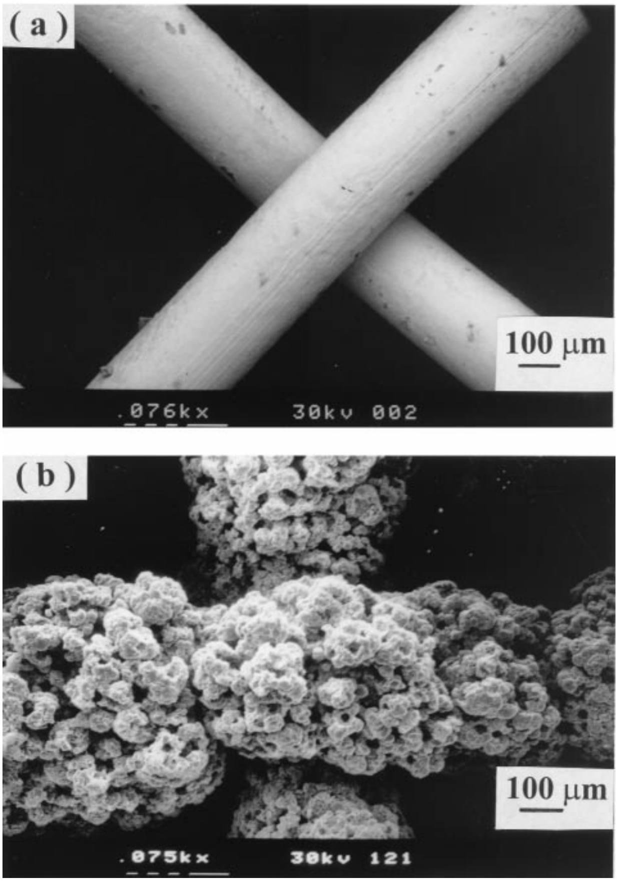

FIG. 3
SEM micrographs of (a) the bare Ni-mesh wires before electroplating and (b) the Ni coating on the Ni-mesh cathode after electroplating through polyHIPE and subsequent polymer burnout. Electroplating at 35 mAcm^{-2} for 24 h.

straightforward matrix–product relationship between the polymer template and the metal grown through its pores. For the latter to hold, the metal deposit should have been organized in simple spherical aggregates of 10–30 μm (size of the polymer cells) filling the polymer void completely. Instead, it seems that the distortion of the homogeneity of the electric field around the cathode substrate, which is caused by the presence of the insulating PHP shield, gives the Ni deposit its structure. The uneven growth of metal deposits produced by electroplating through porous materials is a common feature of this method for reticulated metal production, and it has recently been modeled [14] in terms of uneven current distribution within porous electrodes.

Figure 4(a) and (b), which show SEM micrographs of the same deposit at higher magnifications, further support this suggestion. In the center of Figure 4(a), a large porous aggregate (ca. 140 μm diameter) consisting of smaller aggregates (ca. 10–30 μm diameter) can be seen. The larger of the latter aggregates is comprised of small spherical deposits. The

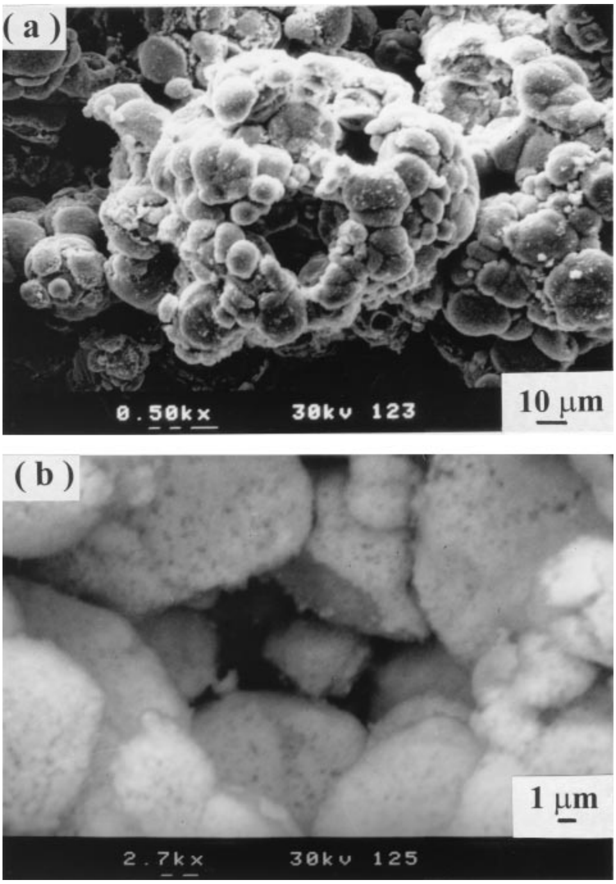

FIG. 4
SEM micrographs of the microporous Ni electrodeposits shown in Figure 3(b).

sequence of events leading to the incorporation of Ni within a single PHP cell could start with the initial growth of the electrodeposit through the pore closer to the cathode substrate and on layers of already deposited Ni in contact with the cell. This deposit could start growing around the pore and into the cell, resulting in one of the smaller spherical structures mentioned above. At moderate current densities (which prevent more extreme field nonhomogeneity), Ni deposits could start entering the cell from neighboring pores further away from the cathode substrate, thus creating more spherical deposits within the individual polymer cell. This description of events takes into account only the local characteristics of the electric field inside a single cell. However, current distribution considerations over the entire electrodeposit growing through a microporous (i.e., locally structured) matrix lead to the conclusion that local current densities vary significantly from pore to pore and from cell to cell, the deposition being favored at locations closer to the facing anode, i.e., at locations that the deposit has already started to build up. This means that the deposition preferentially proceeds around already plated pores, rather than around new pores of the same cell. Once an entire cell is filled with Ni, deposition preferentially starts in a neighboring cell closer to the anode, rather than in one lying at the same plane with the Ni-filled cell. These effects lead to either partially filled or completely void polymer cells in accordance with Figure 4(a), in which 10–30-μm diameter voids can be seen in the body of the central aggregate. In Figure 4(b), much smaller pores of a few microns diameter can be identified between the small spherical aggregates, corresponding to either partial cell filling or the walls of the polymer matrix in the precursor Ni/PHP composite (prior to polymer decomposition). Also, the surface of the aggregates appears to be rough and pitted to a submicron level, probably due to local high current densities resulting in rough deposits and hydrogen embrittlement. These properties should be beneficial to the deposit's catalytic activity, since they increase its true surface area.

A crude estimate of the porosity of the Ni coating can be calculated as follows. From the micrographs in Figure 3(a) and (b), the diameter of the coated Ni wire can be seen to be approximately 750 μm (b) and that of the plain wire, 250 μm (a). The volume of a hypothetical cylindrical nonporous deposit, which can be found by subtracting the volume of the plain wire from that of the coated wire, is 3.93×10^{-3} cm^3/cm of wire. Since there are 10.23 wires per 1 cm along each of the mesh dimensions (mesh specifications: 26×26 wires per inch), it follows that there are $2 \times 10.23 = 20.5$ wires in 1 cm^2 of mesh, amounting to a total wire length of 20.5 cm/cm^2 of mesh. Therefore, a nonporous tubular deposit would have a volume of $3.93 \times 10^{-3} \times 20.5 = 80.565 \times 10^{-3}$ cm^3/cm^2 of mesh. The charge passed during Ni electroplating at 35 mA/cm^2 of mesh for 24 h corresponds to 3,024 C/cm^2 of mesh. The current efficiency as found by weighing the cathode after polymer burnout was ca. 47% (we comment on this value below), which means that $0.47 \times 3{,}024 = 1{,}421$ C were used for Ni electrodeposition per 1 cm^2 of mesh. From Faraday's law (Ni molecular weight and density taken as 58.015 and 8.9 g/cm^3, respectively), we can calculate the actual volume of the Ni deposit to be 48×10^{-3} cm^3/cm^2 of mesh. Therefore, the porosity of the deposit should be approximately $(80.565 - 48)/80.565 = 40.4\%$. The current efficiencies of ca. 50% obtained in all of the Ni-plating experiments through polyHIPE were much lower than the usual 98% values for plating onto bare metal substrates under similar bath, temperature, and current density conditions [26]. This was due to the fact that the local current densities around the polymer pores were much higher than the average current density over the entire sample, resulting in higher rates of hydrogen evolution, competing with nickel deposition and, hence, lowering the efficiency of the latter.

The micrographs in Figure 5 depict situations of partial coating formation due to smaller charges passed through the cell (electroplating at shorter times and/or smaller current densities) and are, therefore, helpful in understanding the development of the microporous structure of the deposit. Close inspection of Figure 5(a) reveals that the initially small spherical deposits are connected to each other by needlelike deposits of submicron width. These very thin deposits, present after only 1 h of electroplating at 33 mA/cm^2, could have been developed through the pores at the walls of neighboring cells, linking small deposits formed within different cells; as time lapses, both the spherical deposits and the Ni needles thickened to finally form structures similar to those shown in Figures 3 and 4. The micrographs in Figure 5(b) and (c), which correspond to very small quantities of electrodeposited Ni, show the first stages of the coating built up where the density of Ni aggregates was small. In particular, Figure 5(c) reveals that, before the first aggregates started to form, the surface of the Ni wire was covered by a rough but nonporous thin Ni layer similar to that sometimes observed on bare metal substrates. It was only after this layer had formed that the deposits started to squeeze into the polymer matrix and, hence, acquired the porous structure discussed

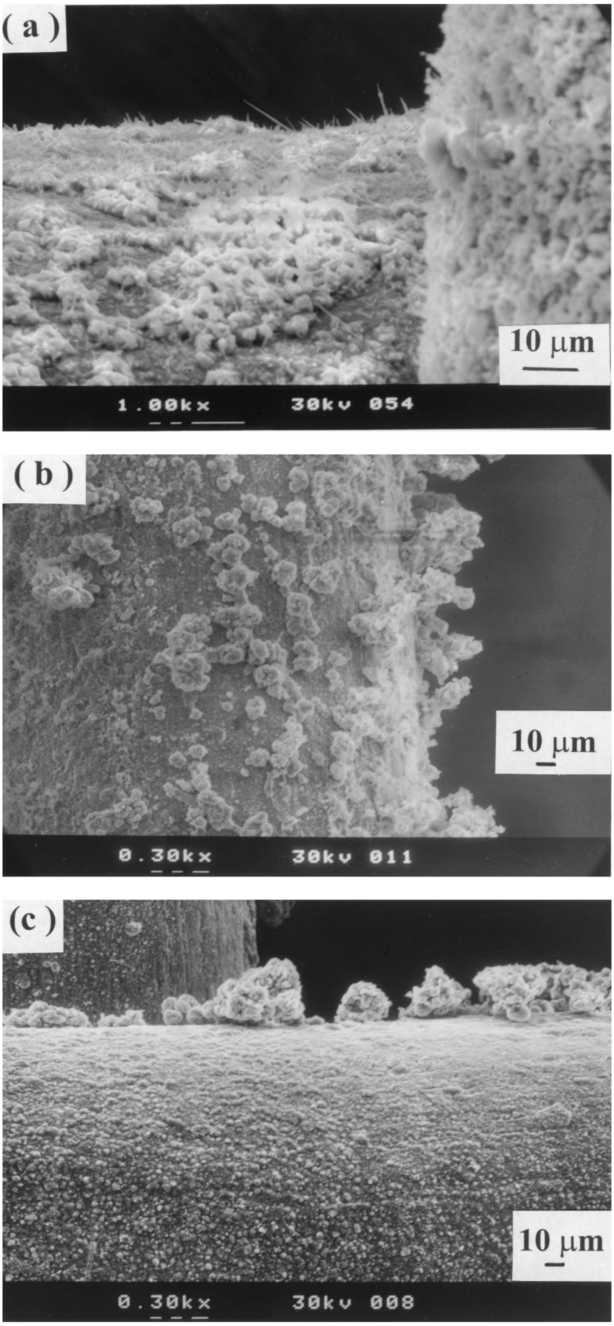

FIG. 5
SEM micrographs of microporous Ni electrodeposits produced after electroplating at (a) 33 mAcm^{-2} for 1 h, (b) 3.3 mAcm^{-2} for 10 min, and (c) same as in (b) but at a different location.

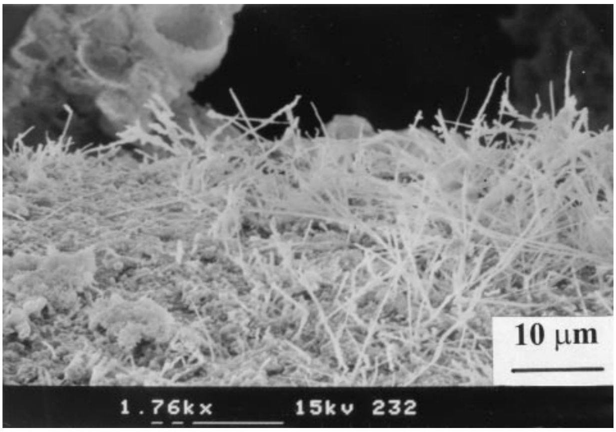

FIG. 6
SEM micrograph of microporous Ni electrodeposits produced after electroplating at 330 mAcm^{-2} for 10 min.

above. This agrees with the fact that polyHIPE is known to not adhere well on metal substrates [22].

Finally, Figure 6 shows the structure obtained when electroplating was carried out at the high current density of 330 mA/cm^2 for 10 min. It can be seen that instead of the granular structure obtained at lower current densities, the deposit consisted of numerous Ni needles of submicron width, probably corresponding to deposits growing only through pores due to a much more nonuniform current distribution at the much higher local current densities prevailing in this case.

ACKNOWLEDGMENTS

The authors wish to thank EPSRC for a studentship to I.J.B. (Quota Ref. No. 97309830). S.S. acknowledges The University of Nottingham for a New Lecturers' Research Grant (97NLRG860) and the Royal Society for a Royal Society Research Grant (RSRG19058).

REFERENCES

1. T.C. Benjamin, E.H. Camera, and L.G. Marianowski, *Handbook of Fuel Cells*, Institute of Gas Technology, Chicago, IL (1980).
2. S. Ye, A.K. Vijh, and L.H. Dao, *J. Electrochem. Soc.* **144**, 90 (1997).
3. Sleem-Ur-Rahman, M.A. Al-Saleh, A.S. Al-Zakri, and S. Gultekin, *J. Appl. Electrochem.* **27**, 215 (1997).
4. O. Böhme, F.U. Leidich, H.J. Salge, and H. Wendt, *Int. J. Hydrogen Energy* **19**, 349 (1994).
5. C.A. Vincent and B. Scrosati, *Modern Batteries*, 2nd ed., Arnold, London (1997).
6. J. Francisco, D. Chiappetti, and J. Brill, in *1996 NASA Aerospace Battery Workshop*, ed. J.C. Brewer, p. 283, NASA Space Flight Center, Huntsville, AL (1997).
7. K. Wall, *Modern Chlor-Alkali Technology*, Vol. 3, Ellis Horwood, Chichester (1986).
8. K. Lohrberg and P. Kohl, *Electrochim. Acta* **29**, 1557 (1984).

9. D.A. Cox, PhD Thesis, Southampton, UK (1981).
10. J. Chaussard, R. Rouget, and M. Tassin, *J. Appl. Electrochem.* **16**, 803 (1986).
11. C.J. Brown, D. Pletcher, F.C. Walsh, J.K. Hammond, and D. Robinson, *J. Appl. Electrochem.* **24**, 95 (1986).
12. S.H. Langer and H.P. Landi, *J. Am. Chem. Soc.* **85**, 3043 (1963).
13. V. Anantharaman and P.N. Pintauro, *J. Electrochem. Soc.* **141**, 2729 (1994).
14. L. Cai and H.Y. Cheh, *Meeting Abstracts of the 191st Meeting of The Electrochemical Society*, p. 58, No. 51, The Electrochemical Society, Inc., Pennington, NJ (1997).
15. H.-D. Kunze, J. Baumeister, J. Banhart, and M. Weber, *PIM* **25**, 182 (1993).
16. S. Ahn and B.J. Tatarchuk, *J. Appl. Electrochem.* **27**, 9 (1997).
17. M. Parent, S. Passerini, B.B. Owens, and W.H. Smyrl, in *Meeting Abstracts of the 191st Meeting of The Electrochemical Society*, p. 840, No. 637, The Electrochemical Society, Inc., Pennington, NJ (1997).
18. Th. Borucinski, S. Rausch, and H. Wendt, *J. Appl. Electrochem.* **22**, 1031 (1992).
19. S. Rausch and H. Wendt, *J. Electrochem. Soc.* **143**, 2852 (1996).
20. D. Barby and Z. Haq, European Patent 0,060,138, Unilever, 1982.
21. J. Williams, *Langmuir* **4**, 44 (1988).
22. G. Akay, Z. Bhumgara, and R.J. Wakeman, *Trans. IChemE* **73**, 782 (1995).
23. P. Hainey, I.M. Huxham, B. Rowatt, D.C. Sherrington, and L. Tetley, *Macromolecules* **24**, 117 (1991).
24. S. Sotiropoulos, I.J. Brown, G. Akay, and E. Lester, *Mater. Lett.* **35**, 383 (1998).
25. F.A. Lowenheim, *Electroplating*, McGraw-Hill, New York (1978).
26. A.K. Graham, *Electroplating Engineering Handbook*, p. 248, Van Nostrand, New York (1971).